IS-PORTO 2023 PROCEEDINGS

Proceedings of the 8th International Symposium on DEFORMATION CHARACTERISTICS OF GEOMATERIALS Porto, 3rd - 6th September 2023

Performance evaluation of the Generalized Bounding Surface Model in the simulation of Cajicá clay subjected to monotonic loading

Ricardo González-Olaya[1], *Javier* Camacho-Tauta[1#], and *Fausto* Molina-Gómez[2]

[1]*Universidad Militar Nueva Granada, Faculty of Engineering, Bogotá, Colombia*
[2] *Universidade do Porto, CONSTRUCT-GEO, Porto, Portugal*
[#]*Corresponding author: javier.camacho@unimilitar.edu.co*

ABSTRACT

Different constitutive models, based on principles of mechanics and experimental evidence, have been developed over several decades to represent and predict the stress-strain behavior of soils subjected to various loading conditions. The Generalized Bounding Surface Model (GBSM) is one of them and is defined as a fully three-dimensional elastoplastic constitutive model for saturated cohesive soils that employ the bounding surface plasticity in conjunction with a non-associative flow rule and a soil microfabric-inspired rotational hardening rule. The GBSM has been successfully validated on numerous laboratory reconstituted soils, but not on natural or undisturbed soil samples. Hence, in this paper the predictive capabilities of the GBSM are evaluated in the simulation of the monotonic behavior of an undisturbed cohesive soil called "Cajicá clay" from the high plain of Bogotá in Colombia. In the first instance, an isotropic consolidation test and a set of axisymmetric triaxial compression and extension tests are conducted using an automated triaxial equipment, to experimentally describe the response of the undisturbed soil. From experimental data, the parameters associated with the GBSM model are calibrated to finally evaluate its capabilities in the simulation of a cohesive natural soil. A comparison between experimental data and numerical simulations is presented to show both performance and advantages of the GBSM model.

Keywords: cohesive soils; soil behavior; numerical simulation; bounding surface plasticity.

1. Introduction

In mechanics, constitutive models are mathematical formulations that describe the stress-strain response of materials (i.e., soils and rocks) subjected to external loadings. Constitutive models for soils, in conjunction with numerical techniques, are used to simulate geotechnical structures and thus analyze and evaluate their behavior and stability. The accuracy and reliability of the results obtained by numerical simulations depend both on the parameters and the predictive capabilities of the models used. Hence, numerous studies have addressed the development of constitutive models to reliably represent and predict the stress-strain-pore pressure behavior of soils subjected to different loading conditions (Potts and Zdravković 1999; Lade 2005; Brinkgreve 2005).

Given that typically soils exhibit elastoplastic behavior, a material response characterized by the simultaneous occurrence of recoverable (elastic) and non-recoverable (inelastic or plastic) strains during loading processes, different theories based on numerous hypotheses have been adopted to formulate elastoplastic soil models (Mendoza and Muniz de Farias 2020).

The Bounding Surface plasticity, developed by Krieg (1975) and Dafalias and Popov (1975), is a plasticity framework that Dafalias et al. (1981) and Dafalias and Herrmann (1982) adapted intending to propose a constitutive model capable of overcoming several limitations in the saturated cohesive soils modelling. The Bounding Surface concept suggests, in contrast to the plasticity theory or "classical" plasticity, that within the surface that encloses stress states that solely produce elastic behavior, an inelastic response can also occur. This assumption, together with other elements developed in the Bounding Surface plasticity, allows simulating a smooth elastoplastic transition that is experimentally evidenced in saturated cohesive soils subjected to monotonic and cyclic loading (Dafalias 1986; 1981).

Considering the Bounding Surface plasticity features, since the 80s different constitutive models based on BS concept have been proposed incorporating new characteristics and consequently providing enhanced predictive capabilities to simulate cohesive soils. Several of these models (e.g., Kaliakin and Dafalias 1989; Ling et al. 2002; Jiang, Ling, and Kaliakin 2012) have been synthesized and improved with Generalized Bounding Surface Model (GBSM) developed by Kaliakin and Nieto-Leal (2013) and Nieto-Leal (2016).

The GBSM, in its most general form, is a Bounding Surface, critical state, fully three-dimensional, rate-dependent model that uses a non-associative flow rule and considers material anisotropy (both inherent and stress induced) through a microfabric-inspired rotational hardening law. GBSM attributes have allowed obtaining satisfactory results simulating an important number of cohesive soils reported in the literature. As shown in

Table 1, based on the data reported by Nieto-Leal and Kaliakin (2014, 2021), Nieto-Leal (2016), Nieto-Leal et al. (2017a, 2017b, 2018, 2020), Kaliakin et al. (2018) and, Kaliakin and Nieto-Leal (2019), most of GBSM simulations correspond to laboratory reconstituted soils, whereby its predictive capabilities in the simulation of undisturbed soils have not been widely explored and evaluated.

Table 1. Cohesive soils simulated using GBSM

Soil	Soil specimens
Soft Bangkok Clay	Undisturbed
Spestone Kaolin	Reconstituted
Bogotá Clay	
Cardiff Kaolin	
Boston Blue Clay	
Lower Cromer Till	
Taipei Silty Clay	
Cambridge Kaolin	
Georgia Kaolin	
Davis Kaolin	
Grundite Clay	
Fujinomori Clay	

This paper aims to assess the GBSM performance in the simulation of the rate-independent monotonic stress-strain-pore pressure behavior of undisturbed Cajicá clay samples using the isotropic non-associative GBSM formulation. Since this model has not been widely explored in clayey soil deposits, a series of undisturbed samples were collected in an experimental site located next to the Center for Studies in Road Infrastructure and Geotechnics located at the Universidad Militar Nueva Granada (in Cajicá) to assess the performance of GMSM in natural conditions. The undisturbed samples were tested in an advanced triaxial equipment that can independently apply radial and axial stresses, allowing for the assessment of soil behavior under any stress-path combination, such as axisymmetric triaxial compression and extension. The tests allowed characterizing the parameters of GBSM. Experimental results were compared against numerical simulations, demonstrating that GBSM represents suitably the behavior of Cajicá clay.

2. Generalized Bounding Surface Model

The GBSM is based on the Bounding Surface concept. This formulation allows the plastic strains to be estimated for stress states that lie within the BS; that is, if the actual stress state of the material is defined in terms of the effective stress tensor σ'_{ij}, stress states within the BS will produce both elastic and plastic strains. On the other hand, in classical plasticity, associated with a yield surface, plastic strains are obtained only when the stress state σ'_{ij} lies above the yield surface, for stress states lying within the yield surface only elastic strains will result.

The GBSM formulation uses elliptical shaped surfaces. In the isotropic non-associative version of the GBSM, the Plastic Potential Surface (Q) and the Bounding Surface (F) are defined by:

$$Q = (\bar{J})^2(R-1)^2 + \frac{M^2}{27}\left(\bar{I} + \frac{R-2}{R}I_0\right)(\bar{I} - I_0) = 0 \quad (1)$$

$$F = (\bar{J})^2(R-1)^2 + \frac{N^2}{27}\left(\bar{I} + \frac{R-2}{R}I_0\right)(\bar{I} - I_0) = 0 \quad (2)$$

where, $I = \sigma'_{kk}$ is the first invariant of the stress tensor σ'_{ij} and $J = \sqrt{1/2\, s_{ij}s_{ij}}$ is the square root of the second invariant of the deviatoric stress tensor $s_{ij} = \sigma'_{ij} - 1/3\sigma'_{kk}\delta_{ij}$; for double subscripts applies the summation law and δ_{ij} is the Kronecker delta. R, N, M are model parameters that configure the shape of Q and F; where, M is the slope of the critical state line in $p' - q$ space and I_0 defines the size of Q and F on the I-axis. The bar over the stress invariants $\bar{I}$ and $\bar{J}$ indicate an "image" point on the Bounding Surface. The values of the real stress invariants I and J are always in or on the surface. For each I and J a unique "image" stress point is assigned by a Mapping Rule such that when the stress state is on the boundary surface $\bar{I} = I$ and $\bar{J} = J$.

The isotropic hardening rule adopted by the GBSM is given by:

$$\dot{I}_0 = \frac{1+e_{in}}{\lambda-\kappa}(\langle I_0 - I_L\rangle + I_L)\dot{\varepsilon}^P_{kk} \quad (3)$$

where λ and κ are critical state parameters, representing the slope of the normal consolidation line (NCL) and κ is the slope of the unloading-reloading lines (URLs) in $e - \ln(p')$ space, respectively. e_{in} is the initial void ratio, I_L is equal to one-third of the atmospheric pressure ($P_a \approx 100\ kPa$), and $\dot{\varepsilon}^P_{kk}$ is the increment in plastic volumetric strain.

The shape hardening function incorporated by the GBSM is:

$$\hat{H} = \frac{1+e_{in}}{\lambda-\kappa}P_a\left[9(F_{,\bar{I}})^2 + \frac{1}{3}\left(F_{,\bar{J}}\right)^2\right][hz^{0.02} + h_0(1 - z^{0.02})]f_n \quad (4)$$

with

$$z = \frac{3\sqrt{3}JR}{NI_0} \quad (5)$$

$$f_n = \frac{1}{2}\left[a + \text{sign}(n_I)(|n_I|)^{\frac{1}{5}}\right]\frac{I}{I_0} \quad (6)$$

$$n_I = \frac{F_{,\bar{I}}}{\sqrt{\left(F_{,\bar{I}}\right)^2 + \left(F_{,\bar{J}}\right)^2}} \quad (7)$$

where $F_{,\bar{I}}$ and $F_{,\bar{J}}$ are the partial derivatives of F with respect to $\bar{I}$ and $\bar{J}$, respectively. h and a are dimensionless model parameters. Further details associated with both model development and fully explicit expressions are presented by Nieto-Leal (2016) and Kaliakin and Nieto-Leal (2017).

3. The Cajicá clay

Cajicá clay is a cohesive material from the Campus of the Universidad Militar Nueva Granada in Cajicá, Colombia. According to the Colombian Geological Survey (2015), the soil deposit is composed of clayey strata, peat and sandy clay separated by sand and gravel lenses. The deposit conformation occurred in the Quaternary period through lacustrine or fluvial-lacustrine deposition processes as indicated by the Van der

Hammen and González (1964) studies. Cohesive materials in this deposit tend to have high compressibility and a high plasticity index as reported by Camacho-Tauta and Reyes-Ortiz (2005), Molina-Gómez et al. (2018), Caicedo et al. (2019), and Ruge et al. (2020).

Undisturbed soil specimens were obtained in the surrounding area of the Center for Studies in Road Infrastructure and Geotechnics located in the Campus (Fig. 1) by subsurface drilling to a depth of 3.0 m, using the thin-walled tube sampling procedure described by the standard practice D1587-08 (ASTM 2008). Samples recovered from the ground exploration were transported to the laboratory and carefully stored to perform physical and mechanical characterization tests, as recommended by Viana da Fonseca et al. (2019). In the following subsections, the results of the physical and mechanical characterization tests are presented.

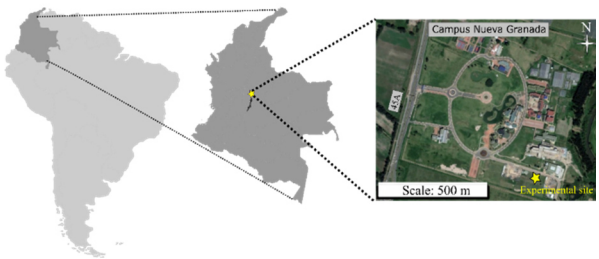

Figure 1. Sampling site location (Ruge et al. 2020).

3.1. Physical properties

For the physical characterization of Cajicá Clay, the procedures established by ASTM standards were used. The liquid limit (LL), plastic limit (PL), and plasticity index (PI) were determined according to standard D4318-10 (ASTM 2010b), the water content (ω_0) by means of the standard D2216-10 (ASTM 2010a), the specific gravity of soil solids (G_s) using the standard D854-10 (ASTM 2010c), and the unit weight (γ) following the standard D7263-09 (ASTM 2009). Cajicá clay was classified as a high plasticity clay (CH) according to the Unified Soil Classification System (USCS) described by the standard practice D2487-17 (ASTM 2017). Physical properties values of Cajicá clay are presented in Table 2.

Table 2. Physical properties of Cajicá clay

G_s [-]	e_0 [-]	ω_0 [%]	LL [%]	IP [%]
2.72	1.594	56.1	81.4	50.5

Note: The initial void ratio (e_0) is estimated with the values of G_s, γ, and ω_0.

3.2. Consolidation characteristics

To characterize the consolidation behavior of the Cajicá clay, a triaxial consolidation test with a loading stage followed by an unloading stage was performed to experimentally define the isotropic consolidation curve. The preconsolidation effective mean stress p'_0 and the critical state parameters λ and κ were determined to describe the isotropic consolidation curve.

Following the Casagrande's method provided by the standard D2435-11 (ASTM 2011b), p'_0 = 320 kPa was estimated. Identifying the NCL and an URL, λ = 0.331 and κ = 0.060 were estimated through fitting.

3.3. Monotonic stress-strain behavior

The Cajicá clay stress-strain behavior and shear strength under monotonic shear was characterized by conducting a series of axisymmetric undrained triaxial compression (TC) and extension (TE) tests.

Using a Wykeham Farrance automated triaxial testing system, cylindrical undisturbed specimens of Cajicá clay were saturated, consolidated and sheared. All specimens were tested with approximate dimensions of 70 mm diameter and 140 mm height, saturated using the back-pressure saturation method ensuring B-parameter values greater than 0.95 with back pressures of at least 300 kPa, and sheared at the strain rate specified by the standard D4767-11 (ASTM 2011a) considering failure at 4% axial strain and time to 50% primary consolidation obtained in the consolidation stage.

Since the mechanical behavior of cohesive soils depends on their stress history, that is, the overconsolidation ratio (OCR), the clay samples tested in compression and triaxial extension were consolidated at isotropic stresses such that specimens with approximate OCR values of 1, 2 and 5.

During undrained compression in the normally consolidated (NC) specimen, the excess pore pressure steadily increases leading the effective stress path to take a leftward direction. In overconsolidated (OC) specimens, the pore pressure increases initially and then it decreases smoothly, causing the effective stress paths turning to the right (Fig. 2a, TC). In the undrained extension of the NC specimen, the excess pore pressure steadily decreases so that the effective stress path is leftward. In contrast, in the OC samples, the pore pressure decreases and then gradually increases resulting in the effective stress paths taking a rightward course (Fig. 2a, TE).

For all OCRs, the Cajicá clay exhibits strain hardening until the failure state where abrupt strain softening (brittle failure) was observed in both compression and extension. Brittle failure occurs for axial strain in range of 3% to 5% in compression and in range of 5% to 10% in extension (Fig. 2b).

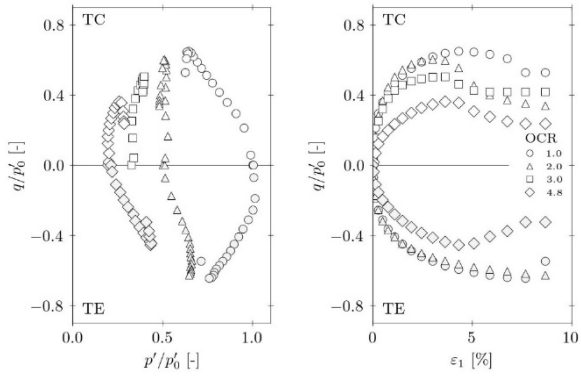

(a) (b)

Figure 2. Undrained Cajicá clay behavior.

In $p' - q$ space, the effective stress paths converge to a well-defined critical state locus (CSL) in both compression and extension paths. Assuming that the CSL is a straight line with slopes M_c and M_e in compression and extension, respectively, by linear regression of the stress states at failure it is established that M_c=1.25 and M_e=0.93. The values of M_c and M_e lead to a single approximate effective friction angle ϕ' of 32.3°.

4. Parameters calibration and model performance

The parameters required by the GBSM model are calibrated by direct comparison between numerical simulations and experimental data from the set of undrained triaxial tests. The calibration of parameters associated with the GBSM was developed considering the recommendations provided by Kaliakin (2005) and following the procedure proposed by Nieto-Leal et al. (2020).

The calibration of the GBSM parameters consisted of: 1) finding the R value in the compression test on a NC sample; 2) adjusting the value of N_e in the extension test on an NC sample with $N_c = M_c$; 3) obtaining the value of C on the family of compression and extension tests on OC samples; and 4) simultaneously capturing the values of h_c, h_e, a and s_p.

The effect of R variation in the simulation of NC specimens is presented in Fig. 3. The value of R=2.38 gave the best simulation of the stress-strain response (correct deviatoric stress at failure) with an accurate evolution of the excess pore pressure, and therefore, a suitable representation of the effective stress path in compression.

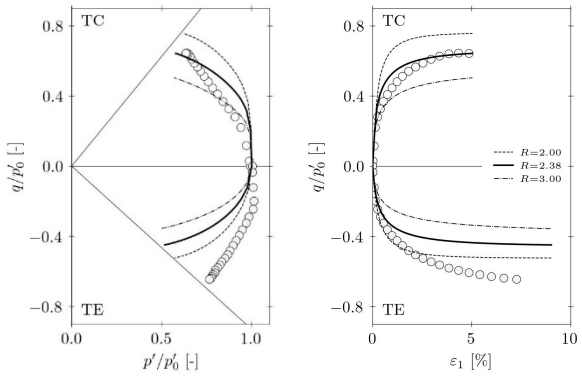

(a) (b)

Figure 3. Calibration of R for Cajicá clay.

N value is calibrated to improve the simulation of NC samples in extension. Since the compression response is correctly simulated, N_c=M_c to avoid modifying the prediction achieved in compression. The value of N_e is varied to reach the best fit in extension, thus, $N_e = 1.58$ allows obtaining a correct simulation of soil behavior. The previously described is evidenced in Fig. 4.

The values of h_c, h_e, a and s_p are calibrated simultaneously to describe with enhanced accuracy the stress-strain behavior and effective stress paths of OC samples. Values of h_c=50, h_e=5, a=3.0, and s_p=1.0 results in the best match between numerical simulations and experimental data.

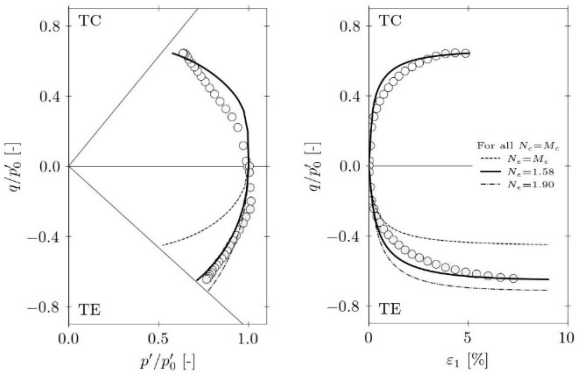

(a) (b)

Figure 4. Calibration of N for Cajicá clay.

Effective stress paths in OC samples are improved by seeking an appropriate C value; hence, several simulations with different C values were carried out. From Fig. 5 it can be established that C = 0.90 yields simulations that better describe the effective stress paths for the family of OC tests considered. Nieto-Leal (2016) reported that numerical issues may occur for C > 0.75; however, in the simulations performed these issues did not occur.

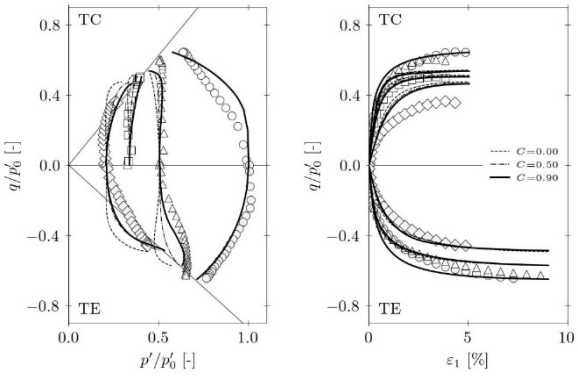

(a) (b)

Figure 5. Calibration of C for Cajicá clay.

The GBSM model parameter values that provide the best accuracy for modelling the Cajicá clay behavior are compiled in Table 3.Simulations of Cajicá clay up to the strain level before brittle failure occurs are presented in Fig. 6 considering the set of GBSM model parameters shown in Table 1.

In compression, the stress-strain behavior and effective stress paths of the samples with OCR values equal to 1.0 and 3.0 are simulated with high accuracy. For OCRs equal to 2.0 and 4.8 there are deficiencies in the simulation of the ultimate deviatoric stress. For OCR = 2.0, the ultimate deviatoric stress is slightly underestimated while for OCR = 4.8 the material strength is overestimated by obtaining ultimate deviatoric stress appreciably higher than that exhibited experimentally. In extension, all the specimens are simulated correctly in general terms. Given the above, it is evident that the use of a non-associative flow rule significantly improves the simulation of Cajicá clay behavior.

Table 3. GBSM model parameters values for Cajicá clay

Parameter	Value
Critical state	
λ	0.331
κ	0.060
M_c	1.25
M_e	0.93
Elasticity	
ν	0.34
Radial mapping rule	
C	0.90
Plastic potential surface	
R	2.38
Bounding surface	
N_c	1.25
N_e	1.58
Shape hardening	
s_p	1.0
h_c	50
h_e	5
a	3.0

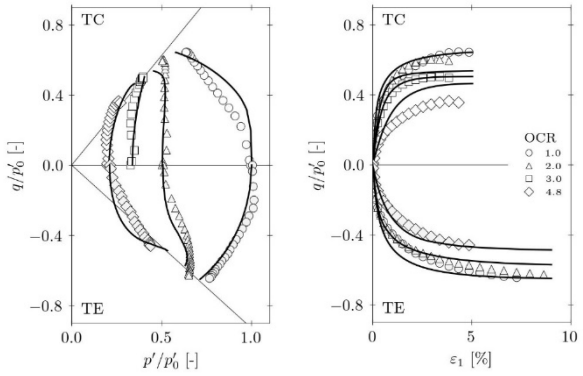

(a) (b)

Figure 6. Simulation of triaxial tests of Cajicá clay using the GBSM.

5. Conclusions

The Generalized Bounding Surface Model was used for the numerical modeling of an undisturbed clay obtained at the Center for Studies in Road Infrastructure and Geotechnics of the Universidad Militar Nueva Granada in Cajicá, Colombia. This clay was physically characterized by conventional laboratory tests and mechanically tested with triaxial equipment. The parameters associated with the GBSM were calibrated with the experimental results of triaxial tests of isotropic consolidation and axisymmetric triaxial compression and extension. Contrasting the experimental results against numerical simulations, it was observed that GBSM can successfully simulate the behavior of the Cajicá clay. It is noteworthy that: 1) the use of a non-associative flow rule significantly improves the prediction of Cajicá clay behavior, particularly the failure state; 2) the model is able to successfully simulate the evolution of excess pore pressure, and hence effective stress paths, during shearing of the Cajicá clay for all overconsolidation ratios; 3) as the overconsolidation ratio increases, the accuracy of the model predictions for simulating the undrained behavior of the Cajicá clay decreases.

Acknowledgements

This research work was developed with the support provided by the Universidad Militar Nueva Granada through the Center for Studies in Road Infrastructure and Geotechnics and the Vice President Office for Research under grant number IMP-ING-2932, this support is gratefully acknowledged.

References

ASTM "Standard Practice for Thin-Walled Tube Sampling of Soils for Geotechnical Purposes (D1587-08)", Annual Book of ASTM Standards, West Conshohocken PA U.S., 2008.

ASTM "Standard Test Methods for Laboratory Determination of Density (Unit Weight) Of Soil Specimens (D7263-09)", Annual Book of ASTM Standards, West Conshohocken PA U.S., 2009.

ASTM "Standard Test Methods for Laboratory Determination of Water (Moisture) Content of Soil and Rock by Mass (D2216-10)", Annual Book of ASTM Standards, West Conshohocken PA U.S., 2010a.

ASTM "Standard Test Methods for Liquid Limit, Plastic Limit, And Plasticity Index of Soils (D4318-10)", Annual Book of ASTM Standards, West Conshohocken PA U.S., 2010b.

ASTM "Standard test methods for specific gravity of soil solids by water pycnometer (D854-10)", Annual Book of ASTM Standards, West Conshohocken PA U.S., 2010c.

ASTM "Standard Test Method for Consolidated Undrained Triaxial Compression Test for Cohesive Soils (D4767-11)", Annual Book of ASTM Standards, West Conshohocken PA U.S., 2011a.

ASTM "Standard Test Methods for One-Dimensional Consolidation Properties of Soils Using Incremental Loading (D2435-11)", Annual Book of ASTM Standards, West Conshohocken PA U.S., 2011b.

ASTM "Standard Practice for Classification of Soils for Engineering Purposes (Unified Soil Classification System) (D2487-17)", Annual Book of ASTM Standards, West Conshohocken PA U.S., 2017.

Brinkgreve, R. "Selection of Soil Models and Parameters for Geotechnical Engineering Application" In: Geo-Frontiers Congress - Calibration of Constitutive Models, Austin TX, United States, 2005, pp.69-98. http://doi.org/10.1061/40771(169)4

Caicedo, B., C., Mendoza, A., Lizcano, F., Lopez-Caballero. "Some Contributions to Mechanical Behaviors of Lacustrine Deposit in Bogotá, Colombia", J Rock Mech Geotech Eng, 11 (4), pp. 837–49, 2019. http://doi.org/10.1016/j.jrmge.2018.12.016

Camacho-Tauta, J., O., Reyes-Ortiz. "Application of Modified Cam-Clay Model to Reconstituted Clays of the Sabana de Bogotá", Rev Ingen de Constr, 20 (1), pp. 0–12, 2005. http://doi.org/10.18359/rcin.1265

Colombian Geological Survey. "Geologic Map of Colombia", [GIS File] Avaliable at: http://www2.sgc.gov.co/MGC/Paginas/gmc_1M2020.aspx , accessed: 01/January/2022.

Dafalias, Y. "Bounding Surface Plasticity I: Mathematical Foundation and Hypoplasticity", J Eng Mech, 112 (9), pp. 966–87, 1986. http://doi.org/10.1061/(ASCE)0733-9399(1986)112:9(966)

Dafalias, Y. "The Concept and Application of the Bounding Surface in Plasticity Theory" In: IUTAM Symposium - Physical Non-Linearities in Structural Analysis, Senlis, France, 1981, pp. 56–63. http://doi.org/10.1007/978-3-642-81582-9_9

Dafalias, Y., L., Herrmann. "Bounding Surface Formulation of

Soil Plasticity." In: Soil Mechanics-Transient and Cyclic Loads, Chichester, United Kingdom, 1982, pp. 253–82.
Dafalias, Y., L., Herrmann, A., Anandarajah. "Cyclic Loading Response of Cohesive Soils Using a Bounding Surface" In: International Conference on Recent Advances in Geotechnical Earthquake Engineering and Soil Dynamics, St. Louis MO, United States, 1981, pp. 139–44. http://doi.org/10.1061/40771(169)10
Dafalias, Y., E. Popov. "A Model of Nonlinearly Hardening Materials for Complex Loading", Acta Mech, 21, pp. 173–92, 1975. http://doi.org/10.1007/BF01181053
Jiang, J., H., Ling, V., Kaliakin. "An Associative and Non-Associative Anisotropic Bounding Surface Model for Clay", Int J Appl Mech, 79 (3), pp. 241–45, 2012. http://doi.org/10.1115/1.4005958
Kaliakin, V. "Parameter Estimation for Time-Dependent Bounding Surface Models for Cohesive Soils" In: Geo-Frontiers Congress - Soil Constitutive Models, Austin TX, United States, 2005, pp. 237–56.
Kaliakin, V., Y., Dafalias. "Simplifications to the Bounding Surface Model for Cohesive Soils", Int J Numer Anal Methods Geomech, 13 (1), pp. 91–100, 1989. http://doi.org/10.1002/nag.1610130108
Kaliakin, V., A., Nieto-Leal. "Details Pertaining to the Generalized Bounding Surface Model for Cohesive Soils: Revised & Expanded", Department of Civil and Environmental Engineering - University of Delaware, United States, Rep.CEE2017, 2017.
Kaliakin, V., A., Nieto-Leal. "Towards a Generalized Bounding Surface Model for Cohesive Soils" In: Poromechanics V - From Blast and Impact Responses of Porous Media to Constitutive Modelling, Vienna, Austria, 2013, pp. 1011–20.
Kaliakin, V., A., Nieto-Leal, M., Mashayekhi. "Modelling the Time and Temperature-Dependent Response of Cohesive Soils in a Generalized Bounding Surface Model", Trans. Infrastruct Geotechnol, 5, pp. 250-286, 2018. https://doi.org/10.1007/s40515-018-0060-3
Kaliakin, V., A., Nieto-Leal. "Simulating The Behavior of Soft Cohesive Soils Using the Generalized Bounding Surface Model", Intl J Comp Civil Struc Eng, 15(3), pp. 55-76, 2019. https://doi.org/10.22337/2587-9618-2019-15-3-55-76
Krieg, R. "A Practical Two Surface Plasticity Theory", Int J Appl Mech, 42 (3), pp. 641–46, 1975. http://doi.org/10.1115/1.3423656
Lade, P. "Overview of Constitutive Models for Soils" In: Geo-Frontiers Congress - Calibration of Constitutive Models, Austin TX, United States, 2005, pp. 1–34. http://doi.org/10.1061/40786(165)1
Ling, H., D., Yue, V., Kaliakin, N., Themelis. "Anisotropic Elastoplastic Bounding Surface Model for Cohesive Soils" J Eng Mech, 128 (7), pp. 748–58, 2002. http://doi.org/10.1061/(ASCE)0733-9399(2002)128:7(748)
Mendoza, C., M., Muniz de Farias. 2020. "Critical State Model for Structured Soil", J Rock Mech Geotech Eng, 12 (3), pp. 630–41, 2020. http://doi.org/10.1016/j.jrmge.2019.12.006
Molina-Gómez, F., J., Ruge, J. Camacho-Tauta. "Spatial Variability of the Sabana de Bogotá Clayed Soil in Reliability of Primary Consolidation Settlements: Study Case Campus Nueva Granada", Ingen Cien, 14 (27), pp. 179–205, 2018. http://doi.org/10.17230/ingciencia.14.27.8
Nieto-Leal, A. "Generalized Bounding Surface Model for Cohesive Soils: A Novel Formulation for Monotonic and Cyclic Loading", PhD, University of Delaware, 2016.
Nieto-Leal, A., V., Kaliakin. "Improved Shape Hardening Function for Bounding Surface Model for Cohesive Soils", J Rock Mech Geotech Eng, 6, pp. 328–337, 2014. http://doi.org/10.1016/j.jrmge.2013.12.006
Nieto-Leal, A., V., Kaliakin. "Additional Insight into Generalized Bounding Surface Model for Saturated Cohesive Soils", Int J Geomech, 21(6), pp. 04021068, 2021. http://doi.org/10.1061/(ASCE)GM.1943-5622.0002012
Nieto-Leal, A., V., Kaliakin, M., Mashayekhi. "Improved Rotational Hardening Rule for Cohesive Soils and Definition of Inherent Anisotropy", Int J Numer Anal Methods Geomech, 42(3), pp. 469–487, 2017a. http://doi.org/10.1002/nag.2750
Nieto-Leal, A., V., Kaliakin, M., Mashayekhi. "Insight Into Rotational Hardening Rules: A New Proposition", In: Poromechanics V - Creep and Plasticity, Paris, France, 2017b, pp. 1077–1082. http://doi.org/10.1061/9780784480779.134
Nieto-Leal, A., V., Kaliakin, T., Molina. "Performance of the Generalized Bounding Surface Model: Simulation of Cohesive Soils Subjected to Monotonic Loading", In: IFCEE - Advances in Geomaterial Modelling and Site Characterization, Orlando FL, United States, 2018, pp. 197–205. https://doi.org/10.1061/9780784481585.020
Nieto-Leal, A., V., Kaliakin, R., González-Olaya. "Investigation of Parameters Associated with the GBSM for Cohesive Soils", Trans. Infrastruct Geotechnol, 7, pp. 496–515, 2020. http://doi.org/10.1007/s40515-020-00124-9
Potts, D., L. Zdravković. "Finite Element Analysis in Geotechnical Engineering: Theory", 1st ed., Thomas Telford Publishing, London, United Kingdom, 1999.
Ruge, J., F., Molina-Gómez, E., Martínez-Rojas, L. Bulla-Cruz, J., Camacho-Tauta. "Measuring the Liquid Limit of Soils Using Different Fall-Cone Apparatuses: A Statistical Analysis", Measurement, 152, pp. 107352, 2020. http://doi.org/10.1016/j.measurement.2019.107352
Van der Hammen, T., E, González. "A Pollen Diagram from the Quaternary of the Sabana de Bogotá (Colombia) and Its Significance for the Geology of the Northern Andes", Neth J Geosci, 43 (3), pp. 113–17, 1964.
Viana da Fonseca, A., C., Ferreira, C., Ramos, F. Molina-Gómez. "The Geotechnical Test Site in the Greater Lisbon Area for Liquefaction Characterisation and Sample Quality Control of Cohesionless Soils", AIMS Geosci, 5 (2), pp. 325–43, 2019. http://doi.org/10.3934/geosci.2019.2.325